Characterization of the potential energy landscape of an antiplasticized polymer

Robert A. Riggleman,[1] Jack F. Douglas,[2] and Juan J. de Pablo[1]
[1]*Department of Chemical and Biological Engineering, University of Wisconsin-Madison, Madison, Wisconsin 53706, USA*
[2]*Polymers Division, National Institute of Standards and Technology, Gaithersburg, Maryland 20899, USA*
(Received 27 February 2007; revised manuscript received 2 May 2007; published 6 July 2007)

The nature of the individual transitions on the potential energy landscape (PEL) associated with particle motion are directly examined for model fragile glass-forming polymer melts, and the results are compared to those of an antiplasticized polymer system. In previous work, we established that the addition of antiplasticizer reduces the fragility of glass formation so that the antiplasticized material is a stronger glass former. In the present work, we find that the antiplasticizing molecules reduce the energy barriers for relaxation compared to the pure polymer, implying that the antiplasticized system has smaller barriers to overcome in order to explore its configuration space. We examine the cooperativity of segmental motion in these bulk fluids and find that more extensive stringlike collective motion enables the system to overcome larger potential energy barriers, in qualitative agreement with both the Stillinger-Weber and Adam-Gibbs views of glass formation. Notably, the stringlike collective motion identified by our PEL analysis corresponds to incremental displacements that occur within larger-scale stringlike particle displacement processes associated with PEL metabasin transitions that mediate structural relaxation. These "substrings" nonetheless seem to exhibit changes in relative size with antiplasticization similar to those observed in "superstrings" that arise at elevated temperatures. We also study the effects of confinement on the energy barriers in each system. Film confinement makes the energy barriers substantially smaller in the pure polymer, while it has little effect on the energy barriers in the antiplasticized system. This observation is qualitatively consistent with our previous studies of stringlike motion in these fluids at higher temperatures and with recent experimental measurements by Torkelson and co-workers.

DOI: 10.1103/PhysRevE.76.011504 PACS number(s): 64.70.Pf, 61.43.Fs, 61.41.+e

I. INTRODUCTION

The addition of a small-molecule solvent to a polymer glass normally leads to a plasticization of the material; the solvent molecules cause a decrease in the glass transition temperature T_g and soften the material in the glass state, i.e., reduce the elastic moduli [1,2]. In some cases, however, the solvent molecules can "antiplasticize" the polymer. That is, the additive can decrease T_g while *increasing* the stiffness of the material in the glass state. Another characteristic of antiplasticized systems is that the average density in the glass state is higher than that of the pure polymer glass. Systems that exhibit this behavior include tricresyl phosphate in polysulfonate [3] and dibutylphthalate in polycarbonate [4]. Little is firmly established about the molecular origins of antiplasticization, although several models have been proposed (discussed below). A better understanding of this phenomenon could contribute to a number of important technological areas, including the reinforcement of nanoscopic polymer structures for use in semiconductor manufacturing [5] and the preservation of proteins and biological materials [6,7].

Almost two decades ago, Vrentas *et al.* [8] proposed a model of antiplasticization based on a free-volume picture, in which antiplasticizer molecules fill the "voids" in a polymer glass. This view was further developed by Ruiz-Treviño and Paul [9], who relaxed some of the assumptions about the diluent properties made in the initial model of Vrentas *et al.* Ngai and co-workers [10,11] invoked a phenomenological coupling model to explain the effects of antiplasticization, without resorting to the free-volume arguments previously employed. In that model, the local, intramolecular relaxations are assumed to be restricted through intermolecular "coupling" of nearby molecules. Ngai *et al.* proposed that antiplasticizer additives increase the amount of coupling required for local relaxations in polycarbonates of bisphenol A doped with polychlorinated biphenyls. More recently, molecular simulations established that antiplasticization is associated with turning a polymer melt into a stronger glass former [12]; antiplasticization also helps reduce the effects of confinement in thin films, and confinement itself has features in common with antiplasticization, such as inducing stronger glass formation [12].

One of the defining features of glass-forming materials is the extremely long relaxation times that arise as T_g is approached from above. Because of such long relaxation times, molecular dynamics (MD) simulations are of a limited use when studying glassy materials below T_g. Monte Carlo (MC) simulations can be used in the vicinity of T_g [13,14], but they require sophisticated algorithms and can only provide structural information. This slowing down of dynamic processes occurs because the system becomes "trapped" in potential energy basins and relaxation can only occur as the system overcomes energy barriers and "jumps" to adjacent basins. Within this view of glass-forming liquids, it is instructive to move away from both MC and MD simulations and to directly examine the nature of the individual transitions on the potential energy landscape (PEL) that are responsible for particle motion. In this approach, one adopts a picture of glass formation in which glasses are characterized in terms of the features of their PEL [15]. Within this framework, the faster β relaxations are taken as individual transitions over local barriers, while the long-time α relaxations occur through a series of "jumps" between larger basins (metabasins) [15–18]. Recent work has shown that several metabasin

transitions are required for the α relaxation to take place [18,19].

The theory of glass formation of Adam and Gibbs [20] proposes that glassy systems relax via cooperative rearrangements, where particles in a localized region move collectively to relax the system. These regions are commonly known as cooperatively rearranging regions (CRRs), and the dynamic slowdown as T_g is approached from above has been attributed to a growing length scale associated with CRRs. Recent simulations and experiments have detected evidence of CRRs [21–24]; simulations have in fact found that CRRs can take the form of large-scale one-dimensional stringlike rearrangements. These strings have been observed in both atomic glasses [21,25] and polymeric glasses [12,23], and they have been shown to be prominent on time scales corresponding to the end of the β relaxation. Note, however, that observations of stringlike cooperativity in previous simulations have been limited to temperatures well *above* T_g, while here we focus on the low-temperature regime of glass formation.

In order to further characterize the effects of antiplasticization on a coarse-grained polymer material, we characterize the PEL and consider the transitions that arise between adjacent minima on the PEL. Transition-state searches have been useful in previous characterizations of the PEL of glassy systems below T_g [26,27]. Here, we perform extensive transition-state searches on minimized configurations of a pure polymeric system and of an antiplasticized polymer, in both bulk and free-standing thin-film configurations. We find that the height of the energy barriers is substantially reduced in the antiplasticized system, implying that smaller energetic barriers must be overcome for such a system to relax. Upon confinement to a thin, free-standing film geometry, the height of the energy barriers that must be overcome to escape a basin is also decreased in the pure polymer, as previously shown [26]. However, in the antiplasticized system, confinement ceases to have an appreciable effect on the barriers. This seems to be in accordance with our previous work (above T_g) showing that film confinement has little effect on the fragility of polymer fluids that have already been antiplasticized. Additionally, we examine the tendency of these systems to relax via stringlike cooperative rearrangements as they move from one minimum to an adjacent one. We find that these systems indeed exhibit one-dimensional correlated stringlike motion during the elementary transitions investigated here, suggesting that a greater degree of cooperativity is generally required in order to overcome larger energy barriers.

Previous works have shown that metabasin transitions (structural relaxation) take place through a series of inherent structure transitions [18]. We identify the stringlike collective motion found in our PEL analysis below with these incremental displacement events occurring during the course of the larger-scale stringlike particle displacements. These "substrings" exhibit changes in relative size similar to the changes observed with antiplasticization on the strings that occur at elevated temperatures [12]. Thus, while the stringlike motion identified from the PEL analysis cannot be identified in a direct way with the stringlike motion that we have characterized earlier in these fluids at elevated temperatures, both of these measures of stringlike motion quantify the extent of cooperative motion of glass-forming liquids, albeit on different time scales. We therefore conclude that the increasing barrier heights associated with larger collective stringlike motion found in our PEL analysis are in qualitative agreement with the Adam-Gibbs model, where the activation energy for relaxation is directly identified with the number of particles involved in a collective displacement.

II. METHODS

A. Model

The model employed in this work consists of a bead-spring polymer chain and various concentrations of smaller, spherical solvent molecules. It has been shown previously that these small solvent molecules antiplasticize this polymer model by decreasing T_g while *increasing* both the shear modulus and the density in the glassy regime [12]. The polymer molecules were modeled as 32-segment chains, where each segment was connected via a stiff harmonic potential. Nonbonded interactions were taken into account using a Lennard-Jones (LJ) potential where both the energy and forces were shifted at $r=r_{cut}$ such that they go smoothly to zero at r_{cut}. For both the polymer and solvent molecules, the ϵ parameter in the LJ potential was taken to be unity, which prevents phase separation. For the pure polymer, σ_p was taken to be unity, while the σ_s for the solvent was 0.5, making the effective radius of the solvent molecules half that of the polymer monomers. The value of r_{cut} was $2.5\sigma_{ij}$, where σ_{ij} is determined from Lorentz-Berthelot combination rules [$\epsilon_{ij}=\sqrt{\epsilon_i\epsilon_j}$ and $\sigma_{ij}=0.5(\sigma_i+\sigma_j)$]. The mass of the polymer monomer was unity, while the mass of the solvent molecules was 0.125, consistent with their relative volumes. The solvent concentration was 5% by mass (30% by mole). The equilibrium bond length for the polymer chains was also unity, thus creating an offset in the minima of the LJ potential and the harmonic bonded potential for a pure polymer system, and it is this offset that promotes glass formation in these systems. This model for a polymer chain has been studied extensively in the recent past [12,26,28–31]. All units in this work are reduced by the LJ parameters of the polymer monomers; i.e., $T=k_BT^*/\epsilon_A$, $E=E^*/\epsilon_A$, where E is the energy and an asterisk (*) represents the unnormalized quantity.

For bulk systems, periodic boundary conditions were employed in all three directions. Thin-film configurations were prepared by beginning with a bulk configuration well above T_g, at $T=0.6$ (T_g for the pure and antiplasticized bulk systems are estimated to be 0.37 and 0.26, respectively) and expanding the simulation box in the z direction to create two free surfaces perpendicular to the z direction. The films were then equilibrated for 2×10^6 time steps using molecular dynamics at constant temperature, where one time step δt was taken as $0.001\tau_{LJ}$ ($\tau_{LJ}=\sqrt{m\sigma^2/\epsilon}$). Periodic boundaries were implemented in the x and y directions.

B. Vibrational density of states and transition-state searches

The vibrational density of states (VDOS) and the transition-state barriers were determined on 600 configurations

that were originally generated at $T=1.5T_g$ for both the pure polymer and antiplasticized blends. The energy of those configurations was minimized using the conjugate-gradient method [32]. Since we wish to compare the bulk systems with the free-standing thin films, where the thickness of the film changes as the system is minimized, we allowed the volume of the bulk systems to change during minimization so that a direct comparison could be made. The obtained densities were well into the glassy regime of the material [12].

At the energy minimum, the potential energy function of the system can be expanded as

$$U(\mathbf{r}) \approx U_0 + 0.5\mathbf{r}\cdot\mathbf{H}\cdot\mathbf{r} + \cdots, \tag{1}$$

where $\mathbf{H}$ is the second derivative, or Hessian, matrix, given by

$$H_{ij} = \frac{\partial^2 U}{\partial r_i \partial r_j}, \tag{2}$$

and U_0 is the energy at the minimum. The system can be viewed as a collection of $3N-3$ uncoupled harmonic oscillators, where three degrees of freedom are lost due to the periodic boundary conditions. The frequencies ω of the harmonic oscillators are the eigenvalues of

$$\mathbf{H}^{\dagger}\cdot\mathbf{x} = \omega^2\mathbf{x}, \tag{3}$$

where $\mathbf{H}^{\dagger}$ is the Hessian matrix calculated in mass-weighted coordinates,

$$H^{\dagger}_{ij} = \frac{\partial^2 U}{\partial q_i \partial q_j} = \frac{1}{\sqrt{m_i m_j}} H_{ij}, \tag{4}$$

where $q_i=\sqrt{m_i}r_i$, and $\mathbf{x}$ are the eigenvectors corresponding to the eigenvalue ω^2. The vibrational density of states represents the probability of finding a frequency of ω and is denoted by $g(\omega)$. At an energy minimum all of the eigenvalues are greater than zero.

The first-order saddle points correspond to the elementary relaxations of a system [26,27]. Previous work has shown that transitions through first-order saddle points using the technique employed here correspond to transitions between inherent structures of the system [26]. These saddle points allow us to characterize the features of the PEL during inherent structure transitions, and it enables us to study the mechanism the system uses to move through configuration space. Recent work has shown that individual transitions between inherent structures can correspond either to the exploration of a single metabasin on the energy landscape or as part of a series of transitions moving the system from one metabasin to an adjacent metabasin [18]. Therefore, the approximate time scale associated with these transitions should correspond to the β-relaxation regime.

We employ an algorithm [33] that is based on the Cerjan-Miller routine for locating first-order saddle points [34], or stationary points on the PEL that have one negative eigenvalue. First, we displace the system by a small amount along the directions of small curvature (smallest eigenvalues). We then implement the transition-state searching algorithm of Baker [33], which minimizes the energy in the direction of each eigenvector except for the lowest one. The energy is maximized along this latter vector until a saddle point is reached. Within the harmonic approximation, this algorithm allows one to walk up a "streambed" on the PEL that corresponds to the lowest eigenmode.

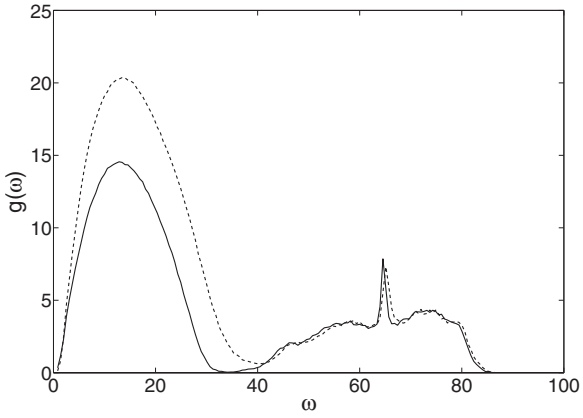

FIG. 1. Vibrational density of states for the pure polymer (solid line) and antiplasticized polymer (dashed line).

Once a transition state has been located, we employ the intrinsic reaction coordinate methodology of Ref. [35]. In this method, we displace our system by a small amount in the positive and negative directions along the eigenvector corresponding to the negative eigenvalue and finally minimize the energy using a steepest-descent algorithm. This yields two energy minima and the first-order transition state that connects the minima. In an attempt to maximize the number of saddle points we explore for our system, for each configuration we attempt four different initial perturbations. This leads to some duplicate transitions, which are discarded. Additionally, any transitions where the starting minimum is not recovered are discarded. After discarding duplicated transitions and those where the initial minimum was not recovered, we obtained at least 1200 saddle points for each system.

III. RESULTS

A. Bulk configurations

The vibrational density of states is shown in Fig. 1 for both the pure and antiplasticized systems. Note that in this figure we have scaled each $g(\omega)$ such that the integral under each curve is $3N$. This enables us to show more directly which frequencies are enhanced by the presence of antiplasticizer particles. There is a clear enhancement of the modes in the range from $\omega=5$ to $\omega=40$. The higher-frequency modes (above $\omega\approx 40$) correspond to the vibrational frequencies of the harmonic bonds in the polymers and remain unaffected by the antiplasticizer. Given that each system has the same number of polymer molecules, it is natural to expect the intensities of each curve to be approximately the same in this frequency range.

A ubiquitous and controversial aspect of glass-forming materials is the excess of frequencies in the range 1 THz $\leqslant\omega\leqslant$ 3 THz compared to the predictions of Debye theory,

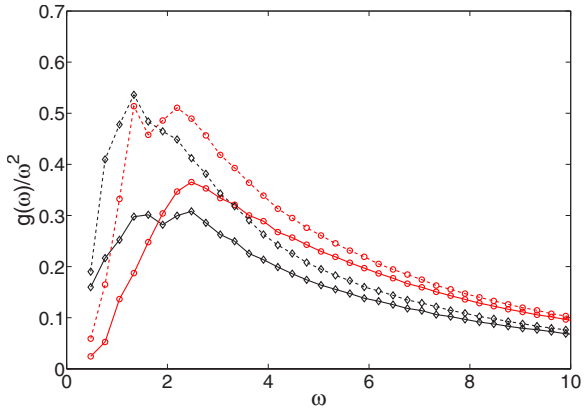

FIG. 2. (Color online) Excess vibrational density of states for the pure polymer (◇) and the antiplasticized systems (○) in both the bulk (solid lines) and thin film (dashed lines) geometries.

where $g(\omega)$ should simply scale as ω^2 [36]. The nature of the modes corresponding to these frequencies, and the cause of the excess frequencies, is a current matter of debate [37–41], although recent work has indicated that it is related to the fluctuations of local elastic constants in glass-forming systems [31,39–41]. The most natural way to observe the excess frequencies is to scale $g(\omega)$ by ω^2, which shows a peak in the part of the frequency range where there are excess modes and Debye theory does not apply. This peak is commonly referred to as the "boson peak." Figure 2 shows the boson peak for our pure and antiplasticized system; evidently, the intensity of the boson peak is *enhanced* by antiplasticization. This appears to be consistent with the view that antiplasticization decreases the fragility of the glass [12]. Previous works have shown that stronger glass-forming materials typically exhibit a more intense boson peak [29,40]. Antiplasticization renders our model a stronger glass former, and the boson peaks in Fig. 2 are consistent with these previous findings [12]. An experimental system exhibiting similar behaviors has been studied by Duval *et al.* [42], where it was found that di(butyl)phthalate enhanced the intensity of the boson peak in poly(methyl methacrylate) below T_g. Duval *et al.* associated this effect with a reduction of the polymer fragility with the addition of the solvent, an effect that we have found in association with antiplasticization [12].

Upon calculating the VDOS, one also obtains the $(3N-3)$ eigenvectors, or normal modes, corresponding to each eigenvalue. Each normal mode contains a displacement vector for all of the particles in the system. We have analyzed the composition of the 5% largest displacement vectors in the antiplasticized system; our aim is to determine whether or not the normal modes of a specific frequency are concentrated on the polymer monomers or the antiplasticizer particles. Figure 3 shows the average composition of the large displacement vectors for the normal modes of each frequency. We find that the low-frequency normal modes concentrate on the antiplasticizer particles. Only the highest frequencies (in the range $40 \leqslant \omega \leqslant 80$) are concentrated on the polymer monomers, and these are the frequencies of the bonds along the polymer backbone. The largest displacements are evidently concentrated on the antiplasticizer particles at a level higher than the overall concentration in the system across most of the ω range.

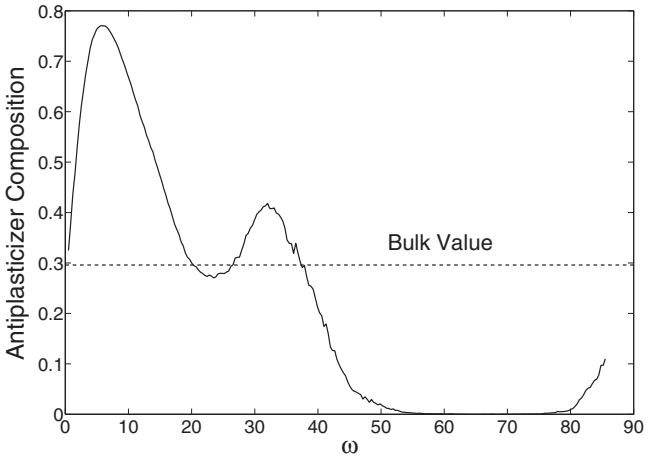

FIG. 3. Composition (mole fraction) of the largest displacement vectors as a function of frequency for the antiplasticized polymer. The overall mole fraction of the system is indicated by the horizontal dashed line.

We now characterize the PEL by studying the energy barriers on the PEL and the relaxation mechanisms as the system moves from one minimum through the saddle point to an adjacent minimum. The height of the energy barriers between the saddle point (SP) and each minimum gives information on how high the barriers are for the system to move through its configuration space. Figure 4 shows the cumulative probability of finding an energy barrier less than ΔU_{bar} as the pure and antiplasticized systems move from the initial minimum M_1 to the SP and from the SP to the second minimum M_2. Antiplasticization lowers the energy barriers on both sides of the saddle point, implying that it is easier for the antiplasticized system to explore configuration space, consistent with the reduction in the scale of collective motion

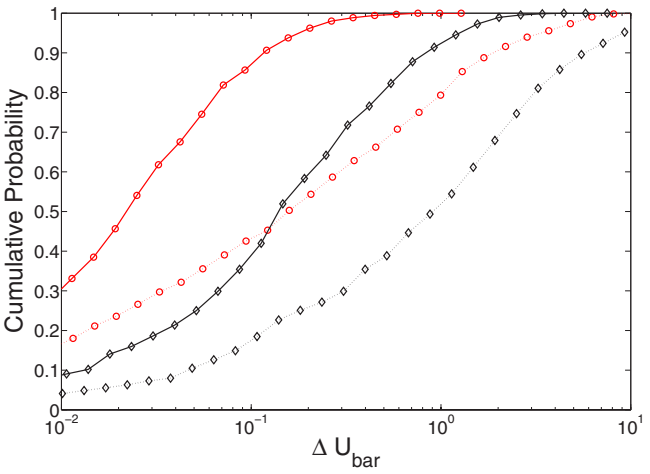

FIG. 4. (Color online) Cumulative probability of finding an energy barrier less than ΔU_{bar} for the pure polymer (◇) and the antiplasticized polymer (○). Solid lines indicate the barrier to escape the initial minimum while dotted lines are for the energy barrier into the second minimum.

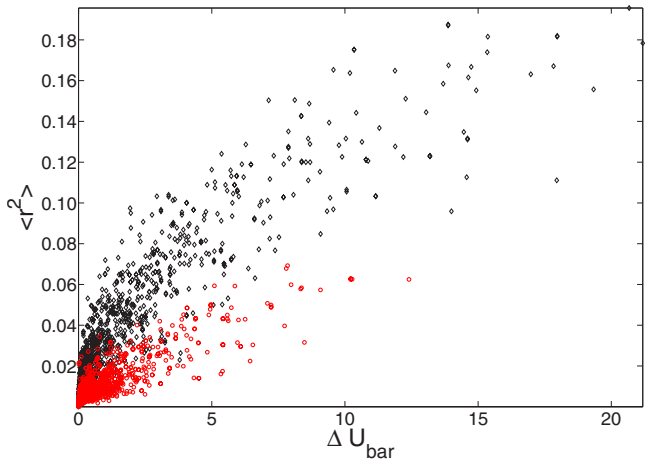

FIG. 5. (Color online) Mean-square displacement $\langle r^2 \rangle$ against the height of the energy barrier as the system moves from a minimum to the saddle point on the PEL. Results for the pure polymer ($\diamond$) and the antiplasticized polymer are shown ($\bigcirc$).

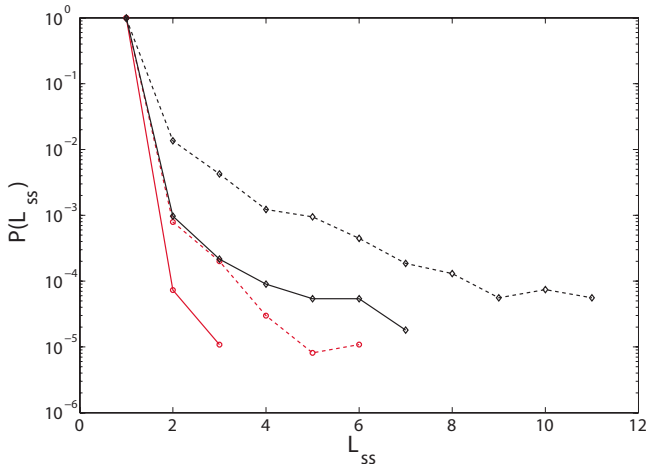

FIG. 6. (Color online) Probability of finding a substring of length $L_s s$ for the pure polymer ($\diamond$) and the antiplasticized polymer ($\bigcirc$) as the system moves from either M_1 to SP (solid lines) or from M_2 to SP (dashed lines).

observed in previous simulations above T_g [12]. In Fig. 4 we also see that the second minima are deeper than the first minima. We attribute this observation to the rapid quench employed in our study, which corresponds to configurations far from equilibrium. We interpret falling into a deeper second minimum as an effect similar to aging, where the inherent structure energy of a glass decreases with aging time. We are currently studying this effect in greater detail in order to determine whether the deeper second minima indeed correspond to a better equilibrated glass.

The next topic of interest involves an attempt to study the mechanism each system uses to overcome its energy barriers. It is natural to expect that the system has to move farther, and possibly in a more cooperative manner, to overcome larger energy barriers; however, these effects have never been considered in detail in previous simulations. We begin by examining the average displacement $\langle r^2 \rangle$ of the entire system as it moves from M_1 or M_2 to the SP. In Fig. 5, we see that there is a strong correlation: higher-energy barriers tend to be associated with larger mean-square displacements. By combining the data from both systems, we find that the correlation coefficient between $\langle r^2 \rangle$ and ΔU_{bar} is 0.85 (95% confidence interval 0.842–0.0858). Additionally, we see from Fig. 5 that the pure polymer requires larger displacements in order to overcome the energy barriers, which is consistent with the picture that more fragile glass formers must move more cooperatively compared to strong glass formers [12,20,43]. We now discuss this point in greater detail.

It has been shown previously that glass-forming materials relax above T_g via collective rearrangements involving forming one-dimensional strings [12,21,23,25]. Above T_g, these strings are defined by analyzing the motion of the particles that have moved farther than the displacements predicted by Brownian motion over a given time window. This time window is usually determined from the maximum in the non-Gaussian parameter for the motion of the particles [12,21], a time that is generally located at the end of the β-relaxation regime. In the present work, however, we do not have an easily accessible time scale to associate with the motion on the PEL. In order to examine stringlike cooperativity, we then examine the most mobile particles as the system moves from either M_1 or M_2 to the SP. We identify stringlike collective motion by investigating the mobile particles in the configurations of our system at a minimum and comparing to those of the saddle point. Next, we look for particles which have replaced the position of adjacent particles. For particles i and j, we determine whether the inequality

$$\min(|\vec{r}_i(M_\alpha) - \vec{r}_j(\mathrm{SP})|, |\vec{r}_j(M_\alpha) - \vec{r}_i(\mathrm{SP})|) < \delta \qquad (5)$$

is satisfied, a condition utilized before in the high-temperature studies of stringlike motion [12,21,23]. If it is satisfied, then the particles are defined as belonging to the same substring. We refer to the strings found in the present calculations as "substrings" in order to make a clear distinction between them and the large-scale stringlike motion quantified in our previous studies of these same fluids above T_g. Here, M_α is either minimum M_1 or M_2 and δ is $0.7\sigma_{ij}$, where σ_{ij} is the σ value associated with the LJ potential between particles i and j. The prefactor in δ is larger here than we have used previously [12]; however, this has no qualitative effect on our results. In the pure polymer system, we examine the most mobile 6.5% of the particles, while in the antiplasticized system we examine the most mobile 23%. This large discrepancy in the percentages has been justified elsewhere and is due to the large difference in mobility between the two components in the antiplasticized system [12]. Given that we find smaller substrings in the antiplasticized system (discussed below), even though we are examining more particles, we feel our approach is justified. Note that isolated mobile particles are designated as substrings with unit length $L_{ss}=1$, consistent with the string definition above T_g [12,21,23].

We have examined the tendency of our system to relax via this mechanism on the PEL, and in Fig. 6 we indicate the

probability of finding a substring of length L_{ss}. We observe that the pure polymer system is much more likely to relax cooperatively than the antiplasticized system, consistent with the behavior above T_g for these systems [12]. When comparing the substring lengths found here to those found above T_g, the strings determined from the PEL analysis are found to be relatively small. This is because the time window associated with *fully developed* stringlike motion above T_g is taken as the maximum in a non-Gaussian parameter. This time, usually denoted by t^*, corresponds to the end of the β relaxation, where a sequence of transitions over local energy barriers have generally taken place [16,18]. The time scale associated with fully developed stringlike motion has been shown to be comparable to the metabasin transition time [19]. Widmer-Cooper and Harrowell have shown [44] that the dynamics on very short time scales, such as the caging time, can be indicative of the dynamics over longer time scales, such as those at the end of the β relaxation. Since the PEL substrings correspond to more local transitions on the PEL, they are naturally less extended than the large-scale strings associated with large-scale structural relaxation. As a consequence, the average string length of the PEL substrings is that their size is close to unity, although this average is a little misleading since the averaging process tends to weigh the noncooperative substrings ($L_{ss}=1$) more heavily. We speculate that a basic difference between substrings and large-scale strings is that the size of the substrings is more reflective of the low-temperature packing characteristics of the material and is thus temperature independent, while the strings themselves exhibit an appreciable temperature dependence as more of these elementary substring events accumulate in the course of the string lifetime. Previous works have shown consistent behaviors using molecular dynamics just above T_g, where it was found that transitions between adjacent inherent structures exhibited smaller strings compared to the transitions between metabasins [18]. As discussed above, the transitions from M_1 to M_2 are analogous to transitions between inherent structures, corresponding to motion during the β relaxation. Also shown in Ref. [18] was the key result that motion over a series of inherent structure transitions was correlated, leading to larger overall strings after successive transitions. While probability distributions such as those reported in Fig. 6 were not shown in Ref. [18], the fraction of the inherent structure transitions which exhibit strings of a given length were shown. If we calculate these fractions for our system, we obtain results that agree with those reported in Ref. [18]. Thus, while we find qualitatively similar behaviors by studying individual transitions compared to MD simulations above T_g, it is difficult to compare these different string definitions on a quantitative level. We would also like to point out that previous works have also observed evidence for cooperativity in the glassy regime [45] using a different definition of cooperativity. Below T_c, it was found that the cluster size was essentially constant. This is an effect that warrants further exploration.

We find that the substrings are longer during the transition from M_2 to the SP compared to the M_1-to-SP transition. Since the energy barriers between M_2 and the SP are larger, this implies that in order to overcome larger energy barriers, not only is the system more mobile overall (Fig. 5), but the motion is more cooperative. This is confirmed in Fig. 7, where the "degree of cooperativity" of the strings, Φ, is plotted against the height of the energy barriers. Here, Φ is the fraction of the mobile particles which are involved in cooperative substrings (i.e., $L_{ss} \geqslant 2$). It is shown that there is a strong correlation between the height of the energy barriers and Φ (correlation coefficient 0.89 with a 95% confidence interval of 0.884–0.896), showing that not only are the displacements larger when overcoming high-energy barriers (Fig. 5), but they are also more cooperative. This is true even for the antiplasticized system, which exhibits less cooperativity than the pure polymer. This is consistent with our previous findings at a higher temperature, where strings in the antiplasticized system were found to be smaller [12], as we would qualitatively expect from the Adam-Gibbs picture of glass formation where larger-scale cooperative motion is associated with growing activation energies [20]. We emphasize again that the cooperative domains in the Adam-Gibbs theory take place on time scales corresponding to metabasin transitions (comparable to the structural relaxation time [18,19] and the lifetime of large stringlike cooperative motion [21]), while this work examines inherent structure transitions associated with the subdynamics of the large-scale motion of the strings. A clear demonstration of the relevance of stringlike motion to metabasin transitions has been made [18]; however, recent work has questioned the relevance of the string mechanism to metabasin transitions [19,46].

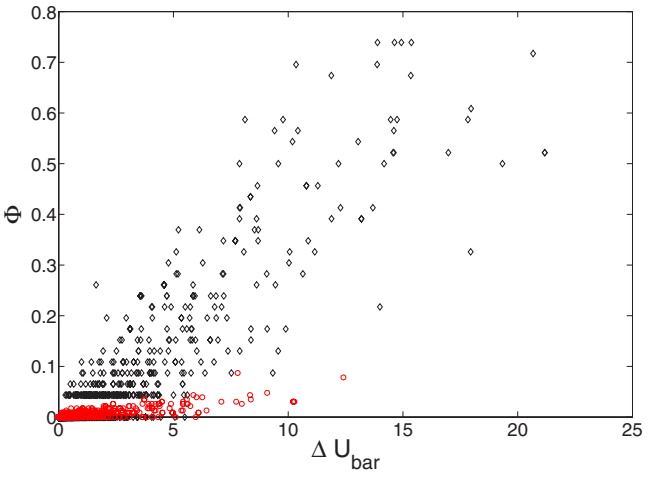

FIG. 7. (Color online) Extent of cooperativity for the pure polymer (◇) and antiplasticized polymer (○) plotted against ΔU_{bar}.

B. Effects of confinement

Previous works have studied the effects of confinement on T_g and the dynamics above T_g [12,47]. It was found that polymeric systems with additives which render the material a stronger glass former (antiplasticization) showed no changes in T_g upon confinement [12,47]. Therefore, it is of interest to study the effects of confinement on the PEL of a pure polymer and a polymeric system containing antiplasticizer particles. First, we compare the effects of confinement on the boson peak. It has been shown that confinement leads to an

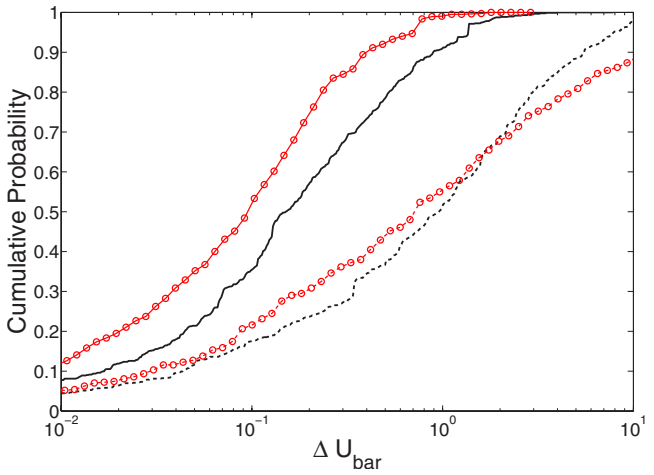

FIG. 8. (Color online) Cumulative probability of finding an energy barrier less than ΔU_{bar} for the pure polymer in the bulk (lines) and thin film geometries (○). Barriers for the M_1-to-SP transition are shown with solid lines; M_2-to-SP transitions are shown with dashed lines.

increase in the intensity of the boson peak [29], which is consistent with a decrease in the fragility of glass formation [40]. Figure 2 shows the boson peaks for both systems in the bulk and thin-film configurations. The effects of confinement on the boson peaks are the same for each system: the intensity of the peak is enhanced, and it is shifted to a lower frequency, which is consistent with previous results on free-standing thin films [29].

Figures 8 and 9 show how confinement alters the height of the energy barriers for both the pure and antiplasticized systems. For the pure polymer systems, the initial energy barriers (from M_1 to the SP) are reduced upon confinement, while the barriers for the second minimum appear to have a broader distribution of values compared to the bulk. This

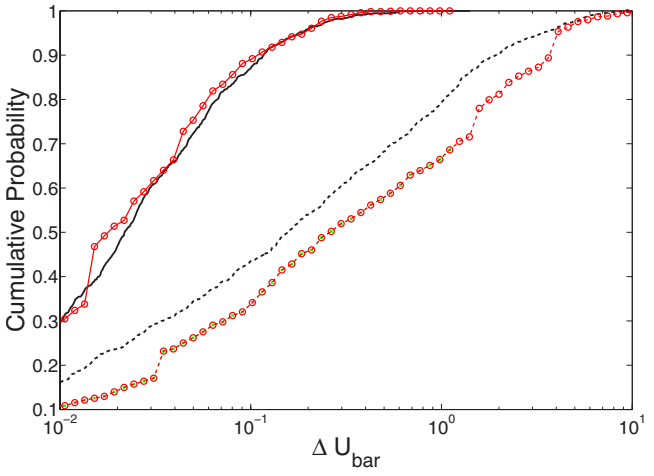

FIG. 9. (Color online) Cumulative probability of finding an energy barrier less than ΔU_{bar} for the antiplasticized polymer in the bulk (lines) and thin-film geometries (○). Barriers for the M_1-to-SP transition are shown with solid lines; M_2-to-SP transitions are shown with dashed lines.

conclusion is made from the observation that the probability for the second barriers on the thin films has a more gradual slope than the bulk system. For the antiplasticized system, shown in Fig. 9, the initial barriers are essentially *unchanged* by confinement. In the bulk material, the initial barriers are decreased upon the addition of antiplasticizer particles and T_g is decreased from 0.37 to 0.26 [12]. Upon confinement of the pure polymer, once again the initial barriers are decreased and T_g is decreased from 0.37 in the bulk to 0.27 in the thin film. However, upon confinement of the antiplasticized system, T_g is unchanged within the simulation uncertainty (0.26 in the bulk to 0.25 in the thin films) and the initial energy barriers are also essentially unchanged (see Fig. 9).

IV. CONCLUSIONS

In summary, we have studied the potential energy landscape of a pure polymer and an antiplasticized polymer in both bulk and thin-film geometries. We find that antiplasticization shifts the distribution of eigenfrequencies in the bulk configurations, leading to an increase in the intensity of the boson peak and a slight increase in the frequency of the boson peak. Upon confinement, the boson peak shifts to a slightly lower frequency and higher intensity in both systems. This behavior is consistent with the view that antiplasticization decreases the fragility of polymer glass formation. Our analysis of the PEL indicates that the size of the energy barrier to escape an initial minimum is also reduced upon confinement of the pure polymer to a film. Confinement, however, has little effect on the escape barriers in the antiplasticized system. This behavior follows the relative changes in T_g for each system upon film confinement, as discussed above. The cooperativity of the motion as the system makes elementary transitions on the PEL in the bulk configurations is expressed in terms of collective local motions of a stringlike nature in the glassy state, although these "substrings" are much smaller compared to strings identified previously for these same fluids above T_g [18]. In addition, the motion is more cooperative as the system overcomes higher-energy barriers. If one adopts the view of glass formation of Stillinger and Weber [48], as one approaches T_g from above, one expects to find larger energy barriers that must be overcome for relaxation to take place, this process ultimately leading to dynamic arrest. A second picture of glass formation, put forth by Adam and Gibbs [20] and in more recent entropy theories of glass-formation [43,49–52], requires that the system move more cooperatively as T is lowered to T_g. This cooperative behavior has been directly observed in numerous previous simulation studies [12,21,23] and experimental studies [22], and has been shown to increase as T approaches T_g. Our results show that overcoming larger energy barriers requires a larger degree of cooperativity, so that the Stillenger-Weber and Adam-Gibbs pictures are both qualitatively consistent with our observations, with the qualification that we are not directly studying the full metabasin transitions. The metabasin transitions governing the α relaxation involve a series of collective (substring) transition events, and in the present work we focus on more el-

ementary displacement subevents based on a PEL analysis. Since the structural relaxation time can be astronomical in the glass state, the substring displacements can be expected to play a significant role in the dynamics of glasses. In particular, we anticipate that these motions might play a significant role in understanding the nonlinear deformation and low-temperature thermodynamic properties of these materials. We are currently exploring this possibility.

ACKNOWLEDGMENTS

This work is supported by the SRC (Grant No. 2005-OC-985) and by the NSF (NIRT Grant No. CTS-0506840).

[1] J. Ferry, *Viscoelastic Properties of Polymers* (Wiley, New York, 1980).
[2] J. M. G. Cowie, *Polymers: Chemistry and Physics of Modern Materials*, 2nd ed. (Thornes, Cheltenham, 1998).
[3] Y. Maeda and D. Paul, J. Polym. Sci., Part B: Polym. Phys. **25**, 957 (1987).
[4] R. Casalini, K. Ngai, C. Robertson, and C. Roland, J. Polym. Sci., Part B: Polym. Phys. **38**, 1841 (2000).
[5] M. P. Stoykovich, H. B. Cao, K. Yoshimoto, L. E. Ocola, and P. F. Nealey, Adv. Mater. (Weinheim, Ger.) **14**, 1180 (2003).
[6] D. P. Miller, R. E. Anderson, and J. J. de Pablo, Pharm. Res. **15**, 1215 (1998).
[7] G. Caliskan, D. Mechtani, J. H. Roh, A. Kisliuk, A. P. Sokolov, S. Azzam, M. Cicerone, S. Lin-Gibson, and I. Peral, J. Chem. Phys. **121**, 1978 (2004).
[8] J. Vrentas, J. Duda, and H. Ling, Macromolecules **21**, 1470 (1988).
[9] F. A. Ruiz-Treviño and D. R. Paul, J. Polym. Sci., Part B: Polym. Phys. **36**, 1037 (1998).
[10] K. L. Ngai, R. W. Rendell, A. F. Yee, and D. J. Plazek, Macromolecules **24**, 61 (1991).
[11] A. K. Rizos, L. Petihakis, K. L. Ngai, J. Wu, and A. F. Yee, Macromolecules **32**, 7921 (1999).
[12] R. A. Riggleman, K. Yoshimoto, J. F. Douglas, and J. J. de Pablo, Phys. Rev. Lett. **97**, 045502 (2006).
[13] R. Faller and J. J. de Pablo, J. Chem. Phys. **119**, 4405 (2003).
[14] Q. Yan, T. S. Jain, and J. J. de Pablo, Phys. Rev. Lett. **92**, 235701 (2004).
[15] M. Goldstein, J. Chem. Phys. **51**, 3728 (1969).
[16] B. Doliwa and A. Heuer, Phys. Rev. E **67**, 031506 (2003).
[17] B. Doliwa and A. Heuer, Phys. Rev. Lett. **91**, 235501 (2003).
[18] M. Vogel, B. Doliwa, A. Heuer, and S. C. Glotzer, J. Chem. Phys. **120**, 4404 (2004).
[19] G. A. Appignanesi, J. A. Rodriguez Fris, R. A. Montani, and W. Kob, Phys. Rev. Lett. **96**, 057801 (2006).
[20] G. Adam and J. Gibbs, J. Chem. Phys. **43**, 139 (1965).
[21] C. Donati, J. F. Douglas, W. Kob, S. J. Plimpton, P. H. Poole, and S. C. Glotzer, Phys. Rev. Lett. **80**, 2338 (1998).
[22] L. Berthier, G. Biroli, J. P. Bouchaud, L. Cipelletti, D. E. Masri, D. L'Hote, F. Ladieu, and M. Perino, Science **310**, 1797 (2005).
[23] M. Aichele, Y. Gebremichael, F. W. Starr, J. Baschnagel, and S. C. Glotzer, J. Chem. Phys. **119**, 5290 (2003).
[24] C. Bennemann, C. Donati, J. Baschnagel, and S. C. Glotzer, Nature (London) **399**, 246 (1999).
[25] V. Teboul, A. Monteil, L. Fai, A. Kerrache, and S. Maabou, Eur. Phys. J. B **40**, 49 (2004).
[26] T. S. Jain and J. J. de Pablo, Phys. Rev. Lett. **92**, 155505 (2004).
[27] N. P. Kopsias and D. N. Theodorou, J. Chem. Phys. **109**, 8573 (1998).
[28] T. S. Jain and J. J. de Pablo, J. Chem. Phys. **122**, 174515 (2005).
[29] T. S. Jain and J. J. de Pablo, J. Chem. Phys. **120**, 9371 (2004).
[30] K. Yoshimoto, T. S. Jain, P. F. Nealey, and J. J. de Pablo, J. Chem. Phys. **122**, 144712 (2005).
[31] K. Yoshimoto, T. S. Jain, K. VanWorkum, P. F. Nealey, and J. J. de Pablo, Phys. Rev. Lett. **93**, 175501 (2004).
[32] W. Press, S. Teukolsky, W. Vetterling, and B. Flannery, *Numerical Recipes in C* (Cambridge University Press, New York, 1988).
[33] J. Baker, J. Comput. Chem. **7**, 385 (1986).
[34] C. J. Cerjan and W. H. Miller, J. Chem. Phys. **75**, 2800 (1981).
[35] K. Fukui, J. Phys. Chem. **74**, 4161 (1970).
[36] D. A. McQuarrie, *Statistical Mechanics* (University Science Books, Sausalito, CA, 2000).
[37] C. A. Angell, J. Phys.: Condens. Matter **16**, S5153 (2004).
[38] C. A. Angell, Y. Yue, L.-M. Wang, J. R. D. Copley, S. Borick, and S. Mossa, J. Phys.: Condens. Matter **15**, S1051 (2003).
[39] F. Léonforte, A. Tanguy, J. P. Wittmer, and J. L. Barrat, Phys. Rev. Lett. **97**, 055501 (2006).
[40] V. N. Novikov, Y. Ding, and A. P. Sokolov, Phys. Rev. E **71**, 061501 (2005).
[41] B. Rossi, G. Viliani, E. Duval, L. Angelani, and W. Garber, Europhys. Lett. **71**, 256 (2005).
[42] E. Duval, M. Kozanecki, L. Saviot, L. David, S. Etienne, V. A. Bershtein, and V. A. Ryzhov, Europhys. Lett. **44**, 747 (1998).
[43] J. Dudowicz, K. F. Freed, and J. F. Douglas, J. Phys. Chem. B **109**, 21350 (2005).
[44] A. Widmer-Cooper and P. Harrowell, Phys. Rev. Lett. **96**, 185701 (2006).
[45] K. Vollmayr-Lee and E. A. Baker, Europhys. Lett. **76**, 1130 (2006).
[46] E. Flenner and G. Szamel, Phys. Rev. E **72**, 011205 (2005).
[47] C. J. Ellison, R. L. Ruszkowski, N. J. Fredin, and J. M. Torkelson, Phys. Rev. Lett. **92**, 095702 (2004).
[48] F. H. Stillinger and T. A. Weber, Phys. Rev. A **28**, 2408 (1983).
[49] J. Dudowicz, K. F. Freed, and J. F. Douglas, J. Chem. Phys. **123**, 111102 (2005).
[50] Y. Singh, J. P. Stoessel, and P. G. Wolynes, Phys. Rev. Lett. **54**, 1059 (1985).
[51] X. Y. Xiz and P. G. Wolynes, Proc. Natl. Acad. Sci. U.S.A. **97**, 2990 (2000).
[52] J. D. Stevenson, J. Schmalian, and P. G. Wolynes, Nat. Phys. **2**, 268 (2006).